galaxies

MDPI

Review

Hot Stars in Stellar Populations of Galaxies

Claus Leitherer

Space Telescope Science Institute, 3700 San Martin Dr, Baltimore, MD 21218, USA; leitherer@stsci.edu

Abstract: Star-forming galaxies are hosts of dominant populations of recently formed, hot, massive stars, which give rise to conspicuous stellar spectral features and provide the ionizing fluxes. Strong outflows of these stars shape their properties. These winds affect the evolution and the output of ionizing radiation, as well as the energy and momentum input in the interstellar medium and the chemical enrichment. Many properties of massive stars become even more extreme at a low metallicity. Owing to the pioneering observations of young, metal-poor stellar populations, both locally with HST and large ground-based facilities and at high redshift with JWST, we are at a key moment to assess our understanding of hot massive stars in these galaxies. Stellar population synthesis is a key tool. I will demonstrate how population models of hot, massive stars help to address some issues at the forefront of current research. The recent advent of new evolutionary and atmosphere models of massive stars probing new parameter space allows us to characterize the properties of nearby and distant populations.

Keywords: massive stars; stellar winds; stellar populations; H II regions; star-forming galaxies; chemical abundances; ultraviolet

1. Motivation

The Milky Way hosts numerous spectacular sites of massive star formation. A famous example is the cluster Trumpler 14 shown in Figure 1. It is the birth place of some of the most massive and hottest stars known, including the O2 If* star HD 93129A ([1]). The relative proximity of Trumpler 14 permits detailed studies of its stellar and interstellar content. The interplay between the stellar photon and mass output and the nebular properties is of particular interest. Ref. [2,3] performed a detailed census of the most massive stars, including their wind properties. They found that the nebular Hα recombination flux accounts for ∼70% of the combined ionizing photon output of the stellar population. Taken at face value, this suggests that about 30% of the photons are either destroyed by dust or escape from the H II region. Powerful stellar winds transfer momentum and energy to the interstellar medium (ISM), whose kinetic energy is ∼30% of the wind energy. Due to the young age of the cluster (<3 Myr), supernovae are not expected to contribute. This value is roughly consistent with analytical models of stellar-wind driven bubbles of [4] who predict the efficiencies of ∼30%, but more recent hydrodynamical models accounting for dissipation by turbulence can lower this value by an order of magnitude ([5]).

Studies like the previously mentioned one provide invaluable insight into the processes governing star formation and the evolution of stars, the ISM, and ultimately the galaxy as a whole. Unfortunately, observational limitations restrict such studies to our nearest neighbors of the local group of galaxies. Spectroscopic observations of individual massive stars in resolved populations beyond distances of a few Myr are out of reach. This is where population synthesis modeling comes into play. Population synthesis models aim to

check for updates

Academic Editors: Sergei Zharikov, Serik Khokhlov and Anatoly Miroshnichenko

Received: 24 January 2025
Revised: 26 February 2025
Accepted: 3 March 2025
Published: 7 March 2025

Citation: Leitherer, C. Hot Stars in Stellar Populations of Galaxies. *Galaxies* **2025**, *13*, 20. https://doi.org/10.3390/galaxies13020020

Copyright: © 2025 by the authors. Licensee MDPI, Basel, Switzerland. This article is an open access article distributed under the terms and conditions of the Creative Commons Attribution (CC BY) license (https://creativecommons.org/licenses/by/4.0/).

predict the photometric, spectroscopic, and chemical properties of stellar systems, as well as their radiative and non-radiative feedback. This method was pioneered by [6] after the advent of modern stellar evolutionary tracks in the Hertzsprung–Russell diagram (HRD). Evolutionary synthesis has relatively few free parameters but its success depends on the reliability of the adopted stellar data and models. These are (i) quantities related to the star-formation process, i.e., the star-formation rate and its time evolution and the stellar mass spectrum, also known as the initial mass function (IMF); (ii) stellar evolution models which provide a prescription for the variation in the luminosity (L), effective temperature ($T_{\rm eff}$), and mass (M) as a function of chemical composition Z, initial mass, and time; (iii) libraries describing the spectrum of each star for any (L,$T_{\rm eff}$,M); (iv) nebular line and continuum emissions; (v) and other effects, such as dust attenuation or geometry. Some of the most popular public model packages are binary_c ([7]), BPASS ([8,9]), CIGALE ([10–12]), FSPS ([13,14]), GALEV ([15,16]), GALAXEV ([17,18]), MILES ([19–21]), PÉGASE ([22,23]), POSYDON ([24]), SLUG ([25,26]), Starburst99 ([27,28]), and STARLIGHT ([29]).

In this review, I will demonstrate how we can attempt to understand the properties of hot-star populations in galaxies whose stellar content is no longer resolvable into individual stars, making use of population synthesis models. Most of the discussion will focus on the local universe but I will try to make connections to the high-redshift universe as well. As a compromise between breadth and depth, I will concentrate on three topics that are currently at the forefront of current research: the existence of very massive stars (VMS), the properties of hot stars in the extreme ultraviolet (EUV), and chemical enrichment induced by massive stars.

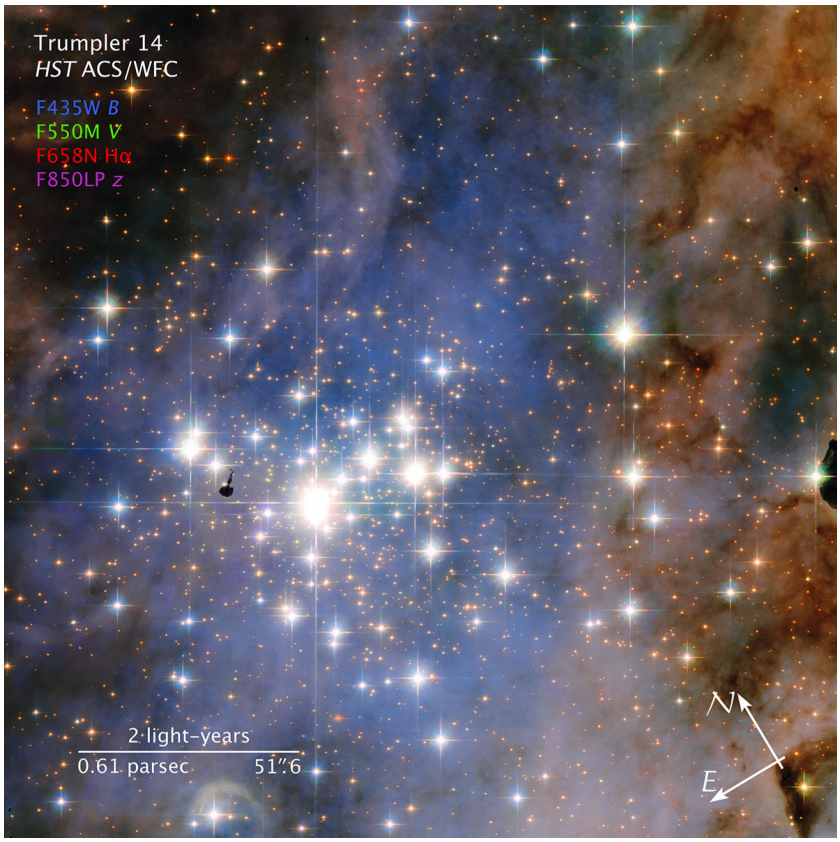


Figure 1. Optical multi-filter HST Advanced Camera for Surveys' composite image of the massive young star cluster Trumpler 14 in the Carina Nebula. Credit: NASA/ESA and J. Maíz Apellániz.

2. The Search for Very Massive Stars

30 Doradus in the Large Magellanic Cloud (LMC) is the most luminous giant H II region in the Local Group ([30]). NGC 2070 is its ionizing star cluster, whose center is designated R136. The innermost region of R136 itself is a dense cluster of massive stars labeled R136a. Ref. [31] found that some of the individual stars of R136 have initial (main-sequence) masses of up to almost 500 $M_\odot$ (Figure 2a). Their analysis used high-quality ground-based and HST spectra and state-of-the-art model atmospheres. Follow-up studies by [32,33] largely confirmed the earlier value and derived a lower limit of ∼250 $M_\odot$ for the initial mass of R136a1. Even accounting for modeling uncertainties, a first convincing case for the existence of VMSs with masses of hundreds of $M_\odot$ has been made. A tell-tale sign (among others) is the strong He II emission line at 1640 and 4686 Å. This line is strong because the stars are hot, He-rich, and have strong stellar winds. The analysis of [31] was done for individual stars. Would we detect these stars in the integrated spectrum of NGC 2070 as well? This is answered in Figure 2b, which reproduces a UV spectrum of the central $2' \times 2'$ of NGC 2070. Whereas the continuum and most other lines are formed in OB and Wolf-Rayet stars, He II 1640 Å comprises R136a, the dense cluster of VMSs. Strong He II and other emission lines can indicate the presence of VMSs.

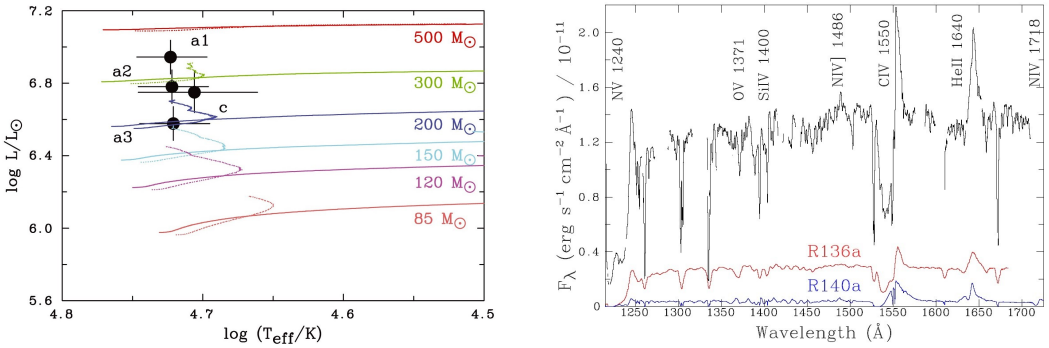


Figure 2. (**a**) HRD with evolutionary tracks showing the location of the four most massive stars in R136, the center of NGC 2070. The stars have initial masses in excess of 200 $M_\odot$ (from [31]). (**b**) Integrated UV spectrum of the central $2' \times 2'$ of NGC 2070 (black); integrated STIS/G140L spectrum of the R136a cluster (red); STIS/E140M spectrum of R140a (blue), the brightest UV star near R136 (from [34]).

Using the UV spectrum of R136a as a template, one can search for evidence of VMSs in more distant young star clusters. This is addressed in Figure 3, where the R136a spectrum is compared to star clusters in four galaxies: (i) Mrk 71, a metal-poor starburst region in the local dwarf galaxy NGC 2366 ([35]); (ii) NGC 5253, which hosts a central young starburst with several massive clusters ([36]); (iii) NGC 3125, known for its extraordinarily strong stellar He II emission ([37]); (iv) the Sunburst Arc, a lensed galaxy at redshift $z = 2.37$ ([38]). The strong similarity of the spectra suggests that all clusters host VMSs.

We can strengthen the evidence of VMSs by performing a spectral synthesis using a spectral library containing the spectra of VMSs. In the past, the UV spectrum of the star cluster NGC 3125-A1 was modeled by [39], who used evolutionary synthesis models of stars with maximum mass of 120 M⊙. This upper limit was imposed by the availability of stellar evolutionary tracks at that time. The models totally failed to reproduce the strong He II 1640 Å emission. Ref. [40] revisited the case, this time using updated models accounting for stars with masses up to 300 $M_\odot$. The result is shown in Figure 4. A model including VMSs with $Z = 0.008$, an age of 2.2 Myr, and a standard Salpeter IMF provided an excellent fit with the He II emission and satisfactorily reproduced almost all other lines.

The agreement between the observed and the modeled spectrum is clear evidence of the presence of VMSs in this star cluster.

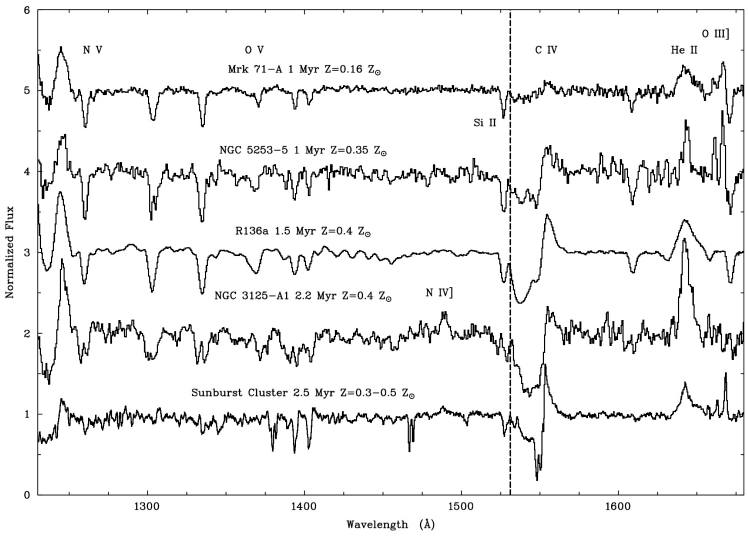


Figure 3. Montage of five UV spectra of massive extragalactic star clusters containing VMSs. The spectra are ordered by increasing age and Z from top to bottom. The spectrum of R136a is identical to that in Figure 2b. The similarity of the R136a spectrum to the other spectra suggests those clusters host VMSs as well (from [35]).

We conclude that there is strong evidence for the existence of very massive stars with masses of several hundred $M_{\odot}$, both as individual stars and in unresolved star-forming regions of galaxies.

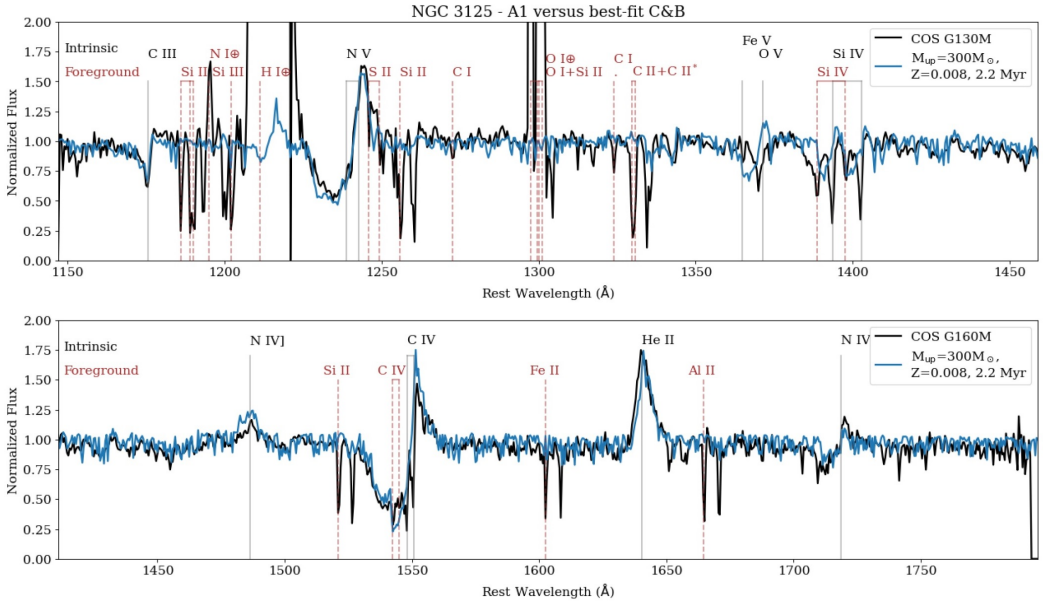


Figure 4. Comparison of a UV spectrum of the star cluster NGC 3125-A1 (black) with a theoretical spectrum containing models of stars with initial masses up to 300 $M_{\odot}$ (blue). The positions of the interstellar intrinsic and foreground, as well as geocoronal lines, are marked. These lines are ignored in the fit (from [40]).

3. Properties of the EUV Radiation Field

Many star-forming galaxies, particularly those with low metallicity, display highly ionized *nebular* emission lines, such as, e.g., C IV 1550 Å and He II 1640 Å, which require ionizing photon energies of 47 eV and 54 eV, respectively ([41]). These lines are narrow and of interstellar origin, and are not to be confused with broad stellar emission lines. No evidence of an active galactic nucleus (AGN) was found in these galaxies; alternative photon sources are required, such as very hot stars, X-ray binaries, or shocks. The VMSs discussed in the previous section appear to be attractive candidates for the emission of such photons. Their large masses and high temperatures place them at the top of the HRD, near the extreme end of the hydrogen main-sequence. Figure 5 compares their location in the HRD to that of other stellar types in the LMC. Stars in the MS-WR group are excellent VMS candidates.

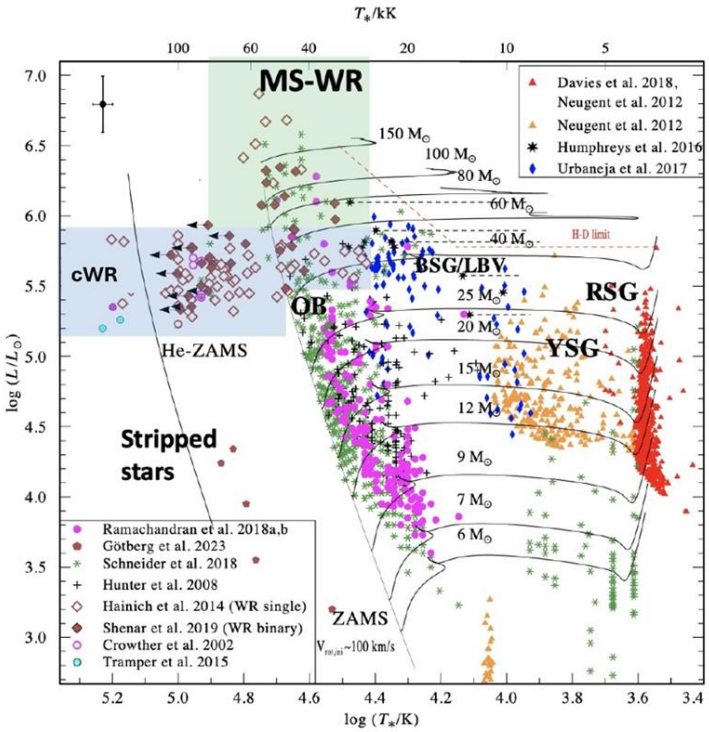


Figure 5. HRD of stellar populations in the LMC. Several key types of stars are identified: main-sequence Wolf-Rayet stars (MS-WR), core-helium burning Wolf-Rayet stars (cWR), OB main-sequence stars (OB), blue supergiants and Luminous Blue Variables (BSG/LBV), red supergiants (RSG), yellow supergiants (YSG), and hydrogen-free stripped stars. Evolutionary tracks and the location of the hydrogen and helium zero-age main sequence are overlaid (from [42]). The references in the figure can be found in [42].

Atmosphere models for the EUV radiation field paint a more complicated picture, as suggested in Figure 6. This figure compares the modeled energy distributions for two stars: an O2 star in the Small Magellanic Cloud (SMC) on the left and the WN5h star R136a1 on the right. R136a1 is one of the VMSs that was previously discussed. While the WN5h star is hotter and bolometrically more luminous than the O2 star, its luminosity in the He^+ ionizing continuum under 228 Å (or above 54 eV) is orders of magnitude lower. This model predicts essentially no flux in this wavelength region. VMSs are close to the Eddington limit, giving rise to strong mass loss and high wind densities. As a result, helium recombines, and the EUV radiation above 54 eV is absorbed in the wind, rather than leaking out and ionizing the ISM.

Returning to Figure 5, we can seek an alternative class of stars. Classical core-helium burning Wolf-Rayet stars (cWR) have long been suspected to be a source of hard EUV photons in metal-poor star-forming galaxies (e.g., [43]). Star-forming galaxies may exhibit both broad He II emissions (indicative of Wolf-Rayet stars) as well as a narrow He II (indicative of hard EUV radiation). An example is the nearby ($D = 3.3$ Mpc) dwarf irregular galaxy NGC 1569. Ref. [44] compared the number of Wolf-Rayet stars and their output of 54^+ eV photons to the recombination-line flux measured in the narrow He II 4686 Å line. Their study suggests that the Wolf-Rayet population can, in principle, meet the required photon budget. However, studies of other galaxies (e.g., [45] for SBS 0335-052) do not support such an agreement. Additional ionization sources may be required, or the stellar models are incomplete. Whereas few galaxies with properties like those of SBS 0335-052 are known locally, nebular He II emission is commonly detected in high-z star-forming galaxies (e.g., [46]), suggesting similar challenges for models.

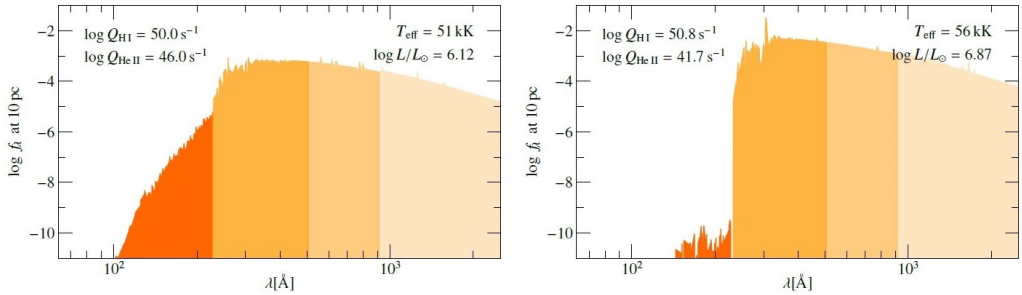


Figure 6. Comparison of the spectral energy distributions of two hot massive stars. The four shaded region in each figure (from light amber to dark red) denote the non-ionizing UV, the H^0-ionizing UV, the He^0-ionizing UV, and the He^+-ionizing UV, respectively. Note the very different He^+-ionizing continuum in the two models (from [47]).

Photo-ionization models can provide more insight into the challenges of modeling the nebular emission lines with the stellar EUV radiation field. Ref. [48] combined stellar-population models from FSPS with CLOUDY ([49]) photo-ionization models to generate a detailed grid of diagnostic diagrams of strategic line ratios. The stellar population barely reaches the observed EUV hardness for extreme ionization parameters and at very short, distinct epochs (4–5 Myr), which seems unlikely to be generally applicable. Considering massive stars stripped of their hydrogen-rich envelopes via binary interaction may significantly harden the spectrum ([50]). The inclusion of these stars in population synthesis models is still incomplete.

Standard stellar population models do not (yet?) reproduce the highest ionization lines emitted by the galactic ISM—even if very massive stars are included.

4. Chemically Enriched Stellar Winds

The winds of massive stars, particularly those of Wolf-Rayet stars, are known to be chemically enriched. This is expected, as winds become stronger and more significant off the main sequence when stars are more luminous, and chemically processed material enters the stellar surface. Wolf-Rayet star winds have been proposed to enrich the surrounding ISM ([51]) but observational evidence is ambiguous. While there are examples of a co-location of Wolf-Rayet stars and nitrogen-enriched ISM gas, such as in NGC 4670 ([52]), there is no statistically significant evidence *local* galaxies hosting Wolf-Rayet stars being systematically overabundant in nebular nitrogen ([53]).

The situation may differ in the more distant universe. The Sunburst Arc is a strongly star-forming galaxy at $z = 2.37$, which is gravitationally lensed by a foreground ($z = 0.44$) galaxy cluster with a magnification factor of 4–80 ([54,55]). A JWST imaging of the Sunburst

Arc is reproduced in Figure 7. A very bright cluster is lensed multiple times, generating 12 images, each of which allow for the restframe UV and optical spectra to be obtained. The resulting optical stacked spectrum obtained with JWST's NIRSpec is plotted in Figure 8. Wolf-Rayet features can clearly be detected. Ref. [56] finds ∼700 Wolf-Rayet stars in the cluster. About 70% are classified as WNh, which are thought to be identical or related to VMSs. The cluster is massive ($M = 9 \times 10^6$ $M_\odot$) and young (age ∼4 Myr), and the associated H II region is highly nitrogen-enriched with log(N/O) = -0.74 ± 0.09 ([56]). This value is above the typical value for local universe H II regions with the same oxygen abundance of 12 + log(O/H) = 7.95. Most likely, VMSs are the main drivers of this nitrogen enhancement. The young age and non-zero metallicity rule out alternative interpretations, such as asymptotic giant branch or Population III stars. There is no evidence for the existence of a black hole, either. A similar suggestion was made regarding the inferred nitrogen overabundance in the very early universe. Galaxies at $z > 10$ have extreme N/O enhancements, similar to that of the Sunburst Arc ([57,58]). This suggests that winds of massive stars, either single or in binaries, may play a crucial role in the production of metals within the first few hundred million years after the big bang.

While nitrogen enrichment in extreme, metal-poor environments appears to be related to winds in hot stars, oxygen enrichment is commonly ascribed to exploding core-collapse supernovae ([59]). Complications arise due to the challenges of modeling the explodability of supernovae ([60]) and the contribution of pair-instability supernovae to the elemental yields ([61]). Oxygen can be used as a proxy for α elements in general. The [α/Fe] versus [Fe/H] relation in a galaxy is one of the most important diagrams in the chemical evolution of galaxies, providing strong constraints on past star-formation activity. [α/Fe] is of particular interest in the high-z universe, where deviations from the local relation are expected. Nebular oxygen abundances are easily accessible and can be assumed to be identical to the stellar abundances due the short lifespan of massive stars. Iron abundances, however, present a challenge. The derived nebular Fe abundances are highly uncertain. Fe condenses on dust grains and is "depleted", requiring large empirical corrections. Furthermore, depletion is variable in star-forming galaxies as supernovae destroy dust and Fe is released ([62]). On the other hand, direct Fe determinations in hot, massive stars are still beyond the state-of-the-art due to the complexity of the Fe transitions.

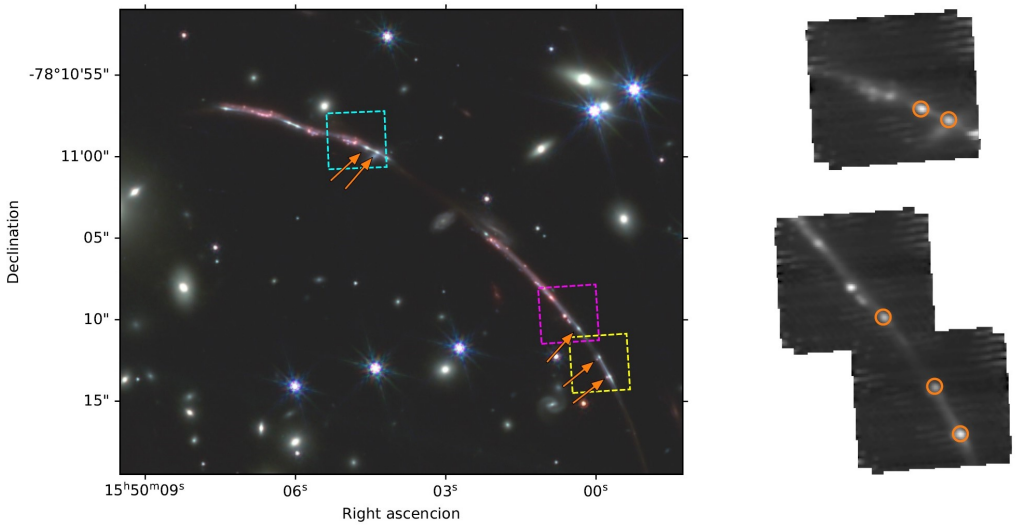


Figure 7. (**Left**): JWST/NIRCam F444W, F200W, and F115W composite image of the Sunburst Arc at $z = 2.37$. The square overlays highlight the locations of the lensed cluster. (**Right**): Close-up of the overlays created from JWST/NIRSpec IFU continuum images (from [56]).

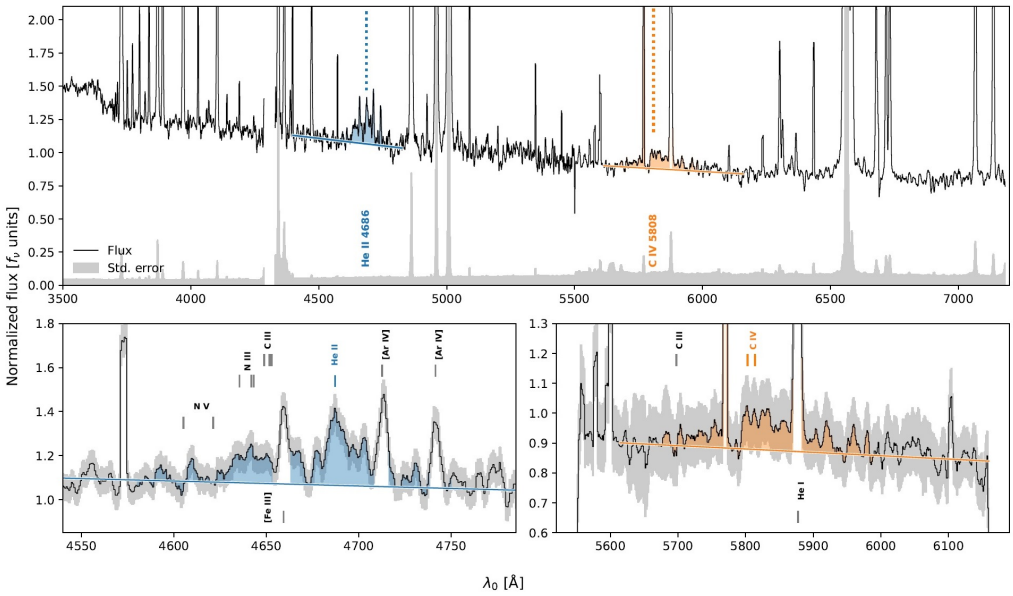


Figure 8. Stacked spectrum of the most massive Sunburst Arc cluster obtained from 12 individual cluster spectra. The broad blue and red Wolf-Rayet emissions of N III/C III/He II 4640/4650/4686 Å and C III 5801/5812 Å, respectively, can be clearly observed (from [56]).

An alternative approach to obtaining stellar Fe abundances in populations dominated by hot stars makes use of the strength of photospheric line-blanketing. The blanketing results from numerous weak lines of mostly Fe^{++}, Fe^{+++} and Fe^{++++}, whose strength varies with the heavy-element abundance ([63,64]). Figure 9 illustrates this method. Ref. [65] derived a stellar Fe abundance of about 0.1 $Z_\odot$ in the stacked spectrum of 30 galaxies at $z = 2.4$. At the same time, a nebular analysis yields a much higher oxygen abundance of about 0.5 $Z_\odot$, suggesting an α/Fe ratio that is enhanced by a factor of 5.

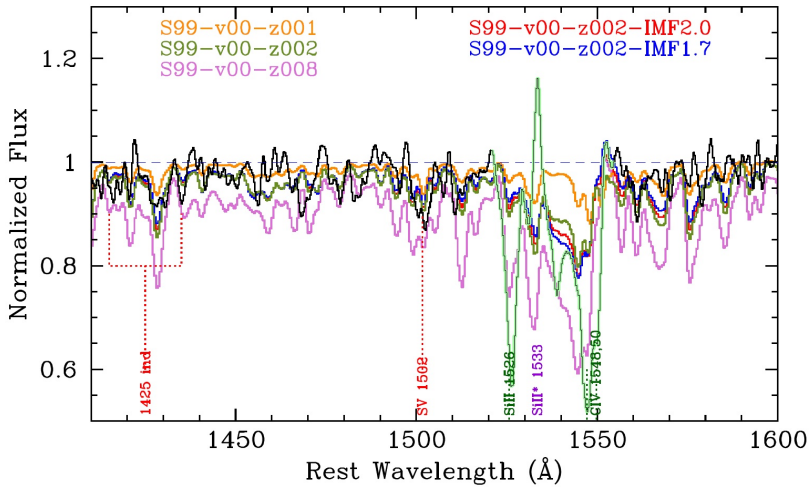


Figure 9. Comparison of a stacked composite restframe UV spectrum of 30 galaxies at redshift $z = 2.4$ (black) with theoretical stellar spectra at three stellar metallicities (0.07 $Z_\odot$, 0.14 $Z_\odot$, 0.56 $Z_\odot$) and two values of the IMF. The variation in the numerous lines superimposed on the continuum is the metallicity-dependent line-blanketing (from [65]).

In combination with the available stellar masses, individual Fe and O abundances allow for studies of the mass-metallicity relation of stars and gas in comprehensive samples of galaxies. A common result in surveys of galaxies at $z = 3 - 4$ is an offset by a factor of 2–5 between the gas-phase and stellar mass–metallicity relation ([66,67]). Core-collapse supernovae enrich the ISM in strongly starbursting galaxies.

The main point of this section is that the ISM of extreme star-forming galaxies at intermediate and high redshifts exhibits evidence of rapid chemical enrichment over a range from a few to hundreds of Myr.

5. Future Perspectives

The past decade has witnessed much-needed progress in our efforts to model hot, massive stars. Both atmosphere and evolution models of stars covering hitherto unexplored parameters have become available. These include stellar models at extreme metallicities, with very high masses and with a fast rotation. Stellar population synthesis is beginning to consistently incorporate such models. Examples of these efforts include, e.g., [68–71]. Notably, stellar evolutionary tracks of supermassive stars ($M > 10^4$ M$_\odot$) that are suitable for population synthesis are still lacking. In Figure 10, we show some results from the latest release of Starburst99. This release covers stellar populations with metallicities ranging from metal-free to supersolar, includes non-rotating and fast-rotating stars, and allows for stars having masses of up to 500 M$_\odot$. The two graphs in this figure show the spectral energy distribution of a single stellar population as a function of time for the first 10 Myr after formation. The figure highlights the impact of VMSs on the EUV and its dependence on metallicity. VMSs boost the hydrogen ionizing continuum prior to reaching their final state. This effect is much enhanced at zero metallicity, when evolution models favor higher stellar temperatures. At the same time, the powerful stellar winds of VMSs amplify the return of mass, momentum, and energy to the galaxy ISM. The complete suite of models from Starburst99 and other population synthesis models will allow us to understand observations of star clusters and galaxies that have so far eluded our interpretation.

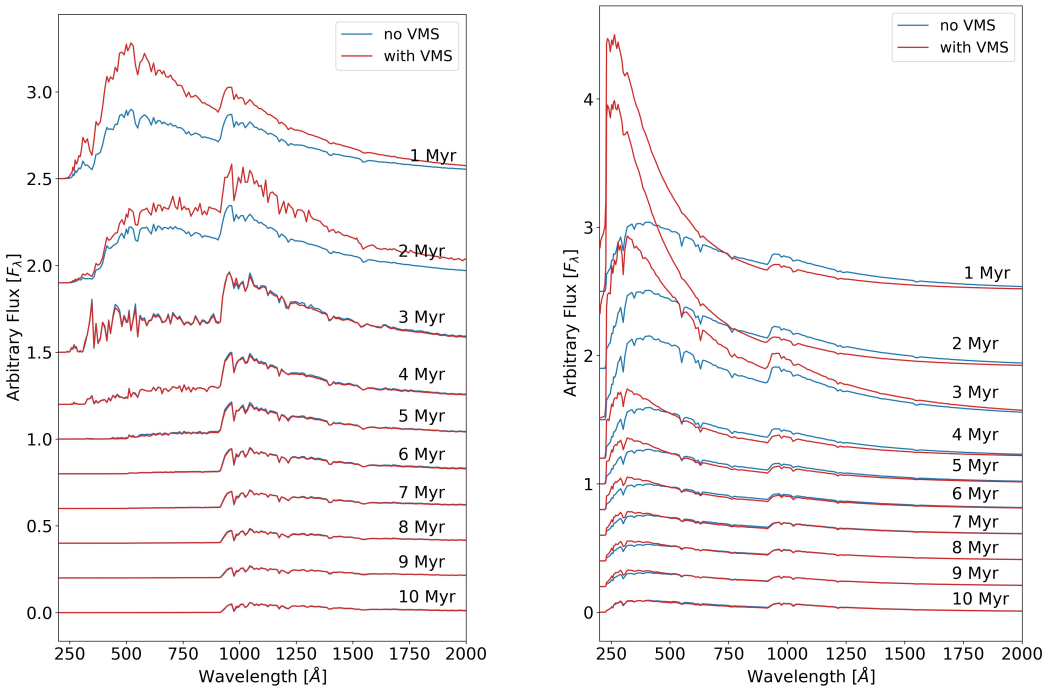


Figure 10. (**a**) Synthetic UV spectral energy distributions for models at a solar metallicity. The evolution over time is plotted from 1 Myr to 10 Myr at intervals of 1 Myr. The models assume a standard Salpeter IMF extending up to 120 M$_\odot$ (blue) and include VMSs with masses of up to 300 M$_\odot$ (red). (**b**) Same as (**a**) but for zero metallicity (from [71]).

Funding: Support for this work was provided by NASA through grant No. AR-16623 from the Space Telescope Science Institute, which is operated by AURA, Inc., under NASA contract NAS5-26555. This research made use of the Astrophysics Data System, funded by NASA under Cooperative Agreement 80NSSC21M00561.

Data Availability Statement: No new data were created or analyzed in this study. Data sharing is not applicable to this article.

Acknowledgments: I would like to thank the organizers of "Hot Stars 2024" for setting up a great conference and for being terrific hosts.

Conflicts of Interest: The author declares no conflicts of interest.

References

1. Morrell, N.I.; Walborn, N.R.; Arias, J.I. A Survey of N IV and O IV Features near 3400 Å in O2-O5 Spectra. *Publ. Astron. Soc. Pac.* **2005**, *117*, 699–705. [CrossRef]
2. Smith, N. A census of the Carina Nebula—I. Cumulative energy input from massive stars. *Mon. Not. R. Astron. Soc.* **2006**, *367*, 763–772. [CrossRef]
3. Smith, N.; Brooks, K.J. A census of the Carina Nebula - II. Energy budget and global properties of the nebulosity. *Mon. Not. R. Astron. Soc.* **2007**, *379*, 1279–1292. [CrossRef]
4. Weaver, R.; McCray, R.; Castor, J.; Shapiro, P.; Moore, R. Interstellar bubbles. II. Structure and evolution. *Astrophys. J.***1977**, *218*, 377–395. [CrossRef]
5. Lancaster, L.; Ostriker, E.C.; Kim, J.G.; Kim, C.G. Efficiently Cooled Stellar Wind Bubbles in Turbulent Clouds. II. Validation of Theory with Hydrodynamic Simulations. *Astrophys. J.* **2021**, *914*, 90. [CrossRef]
6. Tinsley, B.M. Evolution of the Stars and Gas in Galaxies. *Fund. Cosmic. Phys.* **1980**, *5*, 287–388. [CrossRef]
7. Izzard, R. Binary_c: Stellar Population Synthesis Software Framework. Astrophysics Source Code Library. 2023; ascl:2307.035. Available online: https://ui.adsabs.harvard.edu/abs/2023ascl.soft07035I/abstract (accessed on 1 January 2025).
8. Eldridge, J.J.; Stanway, E.R.; Xiao, L.; McClelland, L.A.S.; Taylor, G.; Ng, M.; Greis, S.M.L.; Bray, J.C. Binary Population and Spectral Synthesis Version 2.1: Construction, Observational Verification, and New Results. *Publ. Astron. Soc. Aust.* **2017**, *34*, e058. [CrossRef]
9. Byrne, C.M.; Stanway, E.R.; Eldridge, J.J.; McSwiney, L.; Townsend, O.T. The dependence of theoretical synthetic spectra on α-enhancement in young, binary stellar populations. *Mon. Not. R. Astron. Soc.* **2022**, *512*, 5329–5338. [CrossRef]
10. Burgarella, D.; Buat, V.; Iglesias-Páramo, J. Star formation and dust attenuation properties in galaxies from a statistical ultraviolet-to-far-infrared analysis. *Mon. Not. R. Astron. Soc.* **2005**, *360*, 1413–1425. [CrossRef]
11. Noll, S.; Burgarella, D.; Giovannoli, É.; Serra, P. CIGALE: Code Investigating GALaxy Emission. Astrophysics Source Code Library. 2011; ascl:1111.004. Available online: https://ui.adsabs.harvard.edu/abs/2011ascl.soft11004N/abstract (accessed on 1 January 2025).
12. Boquien, M.; Burgarella, D.; Roehlly, Y.; Buat, V.; Ciesla, L.; Corre, D.; Inoue, A.K.; Salas, H. CIGALE: A python Code Investigating GALaxy Emission. *A&A* **2019**, *622*, A103. [CrossRef]
13. Conroy, C.; Gunn, J.E.; White, M. The Propagation of Uncertainties in Stellar Population Synthesis Modeling. I. The Relevance of Uncertain Aspects of Stellar Evolution and the Initial Mass Function to the Derived Physical Properties of Galaxies. *Astrophys. J.* **2009**, *699*, 486–506. [CrossRef]
14. Conroy, C.; Gunn, J.E. The Propagation of Uncertainties in Stellar Population Synthesis Modeling. III. Model Calibration, Comparison, and Evaluation. *Astrophys. J.* **2010**, *712*, 833–857. [CrossRef]
15. Schulz, J.; Alvensleben, F.-v.U.; Möller, C.S.; Fricke, K.J. Spectral and photometric evolution of simple stellar populations at various metallicities. *A&A* **2002**, *392*, 1–11. [CrossRef]
16. Kotulla, R.; Fritze, U.; Weilbacher, P.; Anders, P. GALEV evolutionary synthesis models—I. Code, input physics and web interface. *Mon. Not. R. Astron. Soc.* **2009**, *396*, 462–484. [CrossRef]
17. Bruzual A.G.; Charlot, S. Spectral Evolution of Stellar Populations Using Isochrone Synthesis. *Astrophys. J.* **1993**, *405*, 538. [CrossRef]
18. Bruzual, G.; Charlot, S. Stellar population synthesis at the resolution of 2003. *Mon. Not. R. Astron. Soc.* **2003**, *344*, 1000–1028. [CrossRef]
19. Vazdekis, A.; Sánchez-Blázquez, P.; Falcón-Barroso, J.; Cenarro, A.J.; Beasley, M.A.; Cardiel, N.; Gorgas, J.; Peletier, R.F. Evolutionary stellar population synthesis with MILES—I. The base models and a new line index system. *Mon. Not. R. Astron. Soc.* **2010**, *404*, 1639–1671. [CrossRef]

20. Vazdekis, A.; Ricciardelli, E.; Cenarro, A.J.; Rivero-González, J.G.; Díaz-García, L.A.; Falcón-Barroso, J. MIUSCAT: Extended MILES spectral coverage—I. Stellar population synthesis models. *Mon. Not. R. Astron. Soc.* **2012**, *424*, 157–171. [CrossRef]
21. Vazdekis, A.; Koleva, M.; Ricciardelli, E.; Röck, B.; Falcón-Barroso, J. UV-extended E-MILES stellar population models: Young components in massive early-type galaxies. *Mon. Not. R. Astron. Soc.* **2016**, *463*, 3409–3436. [CrossRef]
22. Fioc, M.; Rocca-Volmerange, B. PEGASE: A UV to NIR spectral evolution model of galaxies. Application to the calibration of bright galaxy counts. *A&A* **1997**, *326*, 950–962. [CrossRef]
23. Le Borgne, D.; Rocca-Volmerange, B.; Prugniel, P.; Lançon, A.; Fioc, M.; Soubiran, C. Evolutionary synthesis of galaxies at high spectral resolution with the code PEGASE-HR. Metallicity and age tracers. *A&A* **2004**, *425*, 881–897. [CrossRef]
24. Fragos, T.; Andrews, J.J.; Bavera, S.S.; Berry, C.P.L.; Coughlin, S.; Dotter, A.; Giri, P.; Kalogera, V.; Katsaggelos, A.; Kovlakas, K.; et al. POSYDON: A General-purpose Population Synthesis Code with Detailed Binary-evolution Simulations. *Astrophys. J. Suppl. Ser.* **2023**, *264*, 45. [CrossRef]
25. da Silva, R.L.; Fumagalli, M.; Krumholz, M. SLUG—Stochastically Lighting up Galaxies. I. Methods and Validating Tests. *Astrophys. J.* **2012**, *745*, 145. [CrossRef]
26. Krumholz, M.R.; Fumagalli, M.; da Silva, R.L.; Rendahl, T.; Parra, J. SLUG—Stochastically lighting up galaxies-III. A suite of tools for simulated photometry, spectroscopy, and Bayesian inference with stochastic stellar populations. *Mon. Not. R. Astron. Soc.* **2015**, *452*, 1447–1467. [CrossRef]
27. Leitherer, C.; Schaerer, D.; Goldader, J.D.; Delgado, R.M.G.; Robert, C.; Kune, D.F.; de Mello, D.F.; Devost, D.; Heckman, T.M. Starburst99: Synthesis Models for Galaxies with Active Star Formation. *Astrophys. J. Suppl. Ser.* **1999**, *123*, 3–40. [CrossRef]
28. Leitherer, C.; Ekström, S.; Meynet, G.; Schaerer, D.; Agienko, K.B.; Levesque, E.M. The Effects of Stellar Rotation. II. A Comprehensive Set of Starburst99 Models. *Astrophys. J. Suppl. Ser.* **2014**, *212*, 14. [CrossRef]
29. Cid Fernandes, R.; Mateus, A.; Sodré, L.; Stasińska, G.; Gomes, J.M. STARLIGHT: Spectral Synthesis Code. Astrophysics Source Code Library. 2011; ascl:1108.006. Available online: https://ui.adsabs.harvard.edu/abs/2011ascl.soft08006C/abstract (accessed on 1 January 2025).
30. Crowther, P.A. Massive Stars in the Tarantula Nebula: A Rosetta Stone for Extragalactic Supergiant HII Regions. *Galaxies* **2019**, *7*, 88. [CrossRef]
31. Crowther, P.A.; Schnurr, O.; Hirschi, R.; Yusof, N.; Parker, R.J.; Goodwin, S.P.; Kassim, H.A. The R136 star cluster hosts several stars whose individual masses greatly exceed the accepted 150 $M_{\odot}$ stellar mass limit. *Mon. Not. R. Astron. Soc.* **2010**, *408*, 731–751. [CrossRef]
32. Bestenlehner, J.M.; Crowther, P.A.; Caballero-Nieves, S.M.; Schneider, F.R.N.; Simón-Díaz, S.; Brands, S.A.; de Koter, A.; Gräfener, G.; Herrero, A.; Langer, N.; et al. The R136 star cluster dissected with Hubble Space Telescope/STIS-II. Physical properties of the most massive stars in R136. *Mon. Not. R. Astron. Soc.* **2020**, *499*, 1918–1936. [CrossRef]
33. Brands, S.A.; de Koter, A.; Bestenlehner, J.M.; Crowther, P.A.; Sundqvist, J.O.; Puls, J.; Caballero-Nieves, S.M.; Abdul-Masih, M.; Driessen, F.A.; García, M.; et al. The R136 star cluster dissected with Hubble Space Telescope/STIS. III. The most massive stars and their clumped winds. *A&A* **2022**, *663*, A36. [CrossRef]
34. Crowther, P.A.; Castro, N. Mapping the core of the Tarantula Nebula with VLT-MUSE - III. A template for metal-poor starburst regions in the visual and far-ultraviolet. *Mon. Not. R. Astron. Soc.* **2024**, *527*, 9023–9047. [CrossRef]
35. Smith, L.J.; Oey, M.S.; Hernandez, S.; Ryon, J.; Leitherer, C.; Charlot, S.; Bruzual, G.; Calzetti, D.; Chu, Y.H.; Hayes, M.J.; et al. HST FUV Spectroscopy of Super Star Cluster A in the Green Pea Analog Mrk 71: Revealing the Presence of very Massive Stars. *Astrophys. J.* **2023**, *958*, 194. [CrossRef]
36. Smith, L.J.; Crowther, P.A.; Calzetti, D.; Sidoli, F. The Very Massive Star Content of the Nuclear Star Clusters in NGC 5253. *Astrophys. J.* **2016**, *823*, 38. [CrossRef]
37. Chandar, R.; Leitherer, C.; Tremonti, C.A. NGC 3125-1: The Most Extreme Wolf-Rayet Star Cluster Known in the Local Universe. *Astrophys. J.* **2004**, *604*, 153–166. [CrossRef]
38. Meštrić, U.; Vanzella, E.; Upadhyaya, A.; Martins, F.; Marques-Chaves, R.; Schaerer, D.; Guibert, J.; Zanella, A.; Grillo, C.; Rosati, P.; et al. Clues on the presence and segregation of very massive stars in the Sunburst Lyman-continuum cluster at z = 2.37. *A&A* **2023**, *673*, A50. [CrossRef]
39. Wofford, A.; Leitherer, C.; Chandar, R.; Bouret, J.C. A Rare Encounter with Very Massive Stars in NGC 3125-A1. *Astrophys. J.* **2014**, *781*, 122. [CrossRef]
40. Wofford, A.; Sixtos, A.; Charlot, S.; Bruzual, G.; Cullen, F.; Stanton, T.M.; Hernández, S.; Smith, L.J.; Hayes, M. Extreme broad He II emission at high and low redshifts: The dominant role of VMS in NGC 3125-A1 and CDFS131717. *Mon. Not. R. Astron. Soc.* **2023**, *523*, 3949–3966. [CrossRef]
41. Berg, D.A.; Chisholm, J.; Erb, D.K.; Pogge, R.; Henry, A.; Olivier, G.M. Intense C IV and He II Emission in z $\sim$ 0 Galaxies: Probing High-energy Ionizing Photons. *Astrophys. J.* **2019**, *878*, L3. [CrossRef]
42. Shenar, T. Wolf-Rayet stars. *arXiv* **2024**, arXiv:2410.04436. [CrossRef]
43. Schaerer, D. About the Initial Mass Function and He II Emission in Young Starbursts. *Astrophys. J.* **1996**, *467*, L17. [CrossRef]

44. Mayya, Y.D.; Carrasco, E.; Gómez-González, V.M.A.; Zaragoza-Cardiel, J.; Gil de Paz, A.; Ovando, P.A.; Sánchez-Cruces, M.; Lomelí-Núñez, L.; Rodríguez-Merino, L.; Rosa-González, D.; et al. MEGARA-IFU detection of extended He II λ4686 nebular emission in the central region of NGC 1569 and its ionization budget. *Mon. Not. R. Astron. Soc.* **2020**, *498*, 1496–1514. [CrossRef]
45. Kehrig, C.; Vílchez, J.M.; Guerrero, M.A.; Iglesias-Páramo, J.; Hunt, L.K.; Duarte-Puertas, S.; Ramos-Larios, G. The extended He II λ4686 emission in the extremely metal-poor galaxy SBS 0335 – 052E seen with MUSE. *Mon. Not. R. Astron. Soc.* **2018**, *480*, 1081–1095. [CrossRef]
46. Hayes, M.J.; Saldana-Lopez, A.; Citro, A.; James, B.L.; Mingozzi, M.; Scarlata, C.; Martinez, Z.; Berg, D.A. On the Average Ultraviolet Emission Line Spectra of High-Redshift Galaxies: Hot and Cold, Carbon-poor, Nitrogen-modest, and Oozing Ionizing Photons. *arXiv* **2024**, arXiv:2411.09262. [CrossRef]
47. Sander, A.A.C. Massive Stars in the Far and Extreme Ultraviolet. *arXiv* **2022**, arXiv:2211.05424. [CrossRef]
48. Byler, N.; Dalcanton, J.J.; Conroy, C.; Johnson, B.D. Nebular Continuum and Line Emission in Stellar Population Synthesis Models. *Astrophys. J.* **2017**, *840*, 44. [CrossRef]
49. Chatzikos, M.; Bianchi, S.; Camilloni, F.; Chakraborty, P.; Gunasekera, C.M.; Guzmán, F.; Milby, J.S.; Sarkar, A.; Shaw, G.; van Hoof, P.A.M.; et al. The 2023 Release of Cloudy. *Rev. Mex. Astron. Astrofis.* **2023**, *59*, 327–343 . [CrossRef]
50. Götberg, Y.; de Mink, S.E.; Groh, J.H.; Leitherer, C.; Norman, C. The impact of stars stripped in binaries on the integrated spectra of stellar populations. *A&A* **2019**, *629*, A134. [CrossRef]
51. Pagel, B.E.J.; Terlevich, R.J.; Melnick, J. New measurements of helium in H II galaxies. *Publ. Astron. Soc. Pac.* **1986**, *98*, 1005–1008. [CrossRef]
52. Kumari, N.; James, B.L.; Irwin, M.J.; Amorín, R.; Pérez-Montero, E. O/H-N/O: The curious case of NGC 4670. *Mon. Not. R. Astron. Soc.* **2018**, *476*, 3793–3815. [CrossRef]
53. Kobulnicky, H.A.; Skillman, E.D. Elemental Abundance Variations and Chemical Enrichment from Massive Stars in Starbursts. I. NGC 4214. *Astrophys. J.* **1996**, *471*, 211. [CrossRef]
54. Dahle, H.; Aghanim, N.; Guennou, L.; Hudelot, P.; Kneissl, R.; Pointecouteau, E.; Beelen, A.; Bayliss, M.; Douspis, M.; Nesvadba, N.; et al. Discovery of an exceptionally bright giant arc at z = 2.369, gravitationally lensed by the Planck cluster PSZ1 G311.65-18.48. *A&A* **2016**, *590*, L4. [CrossRef]
55. Sharon, K.; Mahler, G.; Rivera-Thorsen, T.E.; Dahle, H.; Gladders, M.D.; Bayliss, M.B.; Florian, M.K.; Kim, K.J.; Khullar, G.; Mainali, R.; et al. The Cosmic Telescope That Lenses the Sunburst Arc, PSZ1 G311.65-18.48: Strong Gravitational Lensing Model and Source Plane Analysis. *Astrophys. J.* **2022**, *941*, 203. [CrossRef]
56. Rivera-Thorsen, T.E.; Chisholm, J.; Welch, B.; Rigby, J.R.; Hutchison, T.; Florian, M.; Sharon, K.; Choe, S.; Dahle, H.; Bayliss, M.B.; et al. The Sunburst Arc with JWST: I. Detection of Wolf-Rayet stars injecting nitrogen into a low-metallicity, z = 2.37 proto-globular cluster leaking ionizing photons. *A&A* **2024**, *690*, A269. [CrossRef]
57. Cameron, A.J.; Katz, H.; Rey, M.P.; Saxena, A. Nitrogen enhancements 440 Myr after the big bang: Supersolar N/O, a tidal disruption event, or a dense stellar cluster in GN-z11? *Mon. Not. R. Astron. Soc.* **2023**, *523*, 3516–3525. [CrossRef]
58. Castellano, M.; Napolitano, L.; Fontana, A.; Roberts-Borsani, G.; Treu, T.; Vanzella, E.; Zavala, J.A.; Arrabal Haro, P.; Calabrò, A.; Llerena, M.; et al. JWST NIRSpec Spectroscopy of the Remarkable Bright Galaxy GHZ2/GLASS-z12 at Redshift 12.34. *Astrophys. J.* **2024**, *972*, 143. [CrossRef]
59. Kobayashi, C. The role of mass loss in chemodynamical evolution of galaxies. In *Proceedings of the International Astronomical Union , Volume 16 , Symposium S366: The Origin of Outflows in Evolved Stars*; Decin, L., Zijlstra, A., Gielen, C., Eds.; Cambridge University Press: Cambridge, UK, 2022; Volume 366, pp. 63–82. [CrossRef]
60. Ebinger, K.; Curtis, S.; Ghosh, S.; Fröhlich, C.; Hempel, M.; Perego, A.; Liebendörfer, M.; Thielemann, F.K. PUSHing Core-collapse Supernovae to Explosions in Spherical Symmetry. IV. Explodability, Remnant Properties, and Nucleosynthesis Yields of Low-metallicity Stars. *Astrophys. J.* **2020**, *888*, 91. [CrossRef]
61. Kozyreva, A.; Blinnikov, S. Can pair-instability supernova models match the observations of superluminous supernovae? *Mon. Not. R. Astron. Soc.* **2015**, *454*, 4357–4365. [CrossRef]
62. Calzetti, D. Reddening and Star Formation in Starburst Galaxies. *AJ* **1997**, *113*, 162–184. [CrossRef]
63. Leitherer, C.; Ortiz Otálvaro, P.A.; Bresolin, F.; Kudritzki, R.P.; Lo Faro, B.; Pauldrach, A.W.A.; Pettini, M.; Rix, S.A. A Library of Theoretical Ultraviolet Spectra of Massive, Hot Stars for Evolutionary Synthesis. *Astrophys. J.S* **2010**, *189*, 309–335. [CrossRef]
64. Cullen, F.; McLure, R.J.; Dunlop, J.S.; Khochfar, S.; Davé, R.; Amorín, R.; Bolzonella, M.; Carnall, A.C.; Castellano, M.; Cimatti, A.; et al. The VANDELS survey: The stellar metallicities of star-forming galaxies at 2.5 < z < 5.0. *Mon. Not. R. Astron. Soc.* **2019**, *487*, 2038–2060. [CrossRef]
65. Steidel, C.C.; Strom, A.L.; Pettini, M.; Rudie, G.C.; Reddy, N.A.; Trainor, R.F. Reconciling the Stellar and Nebular Spectra of High-redshift Galaxies. *Astrophys. J.* **2016**, *826*, 159. [CrossRef]
66. Cullen, F.; Shapley, A.E.; McLure, R.J.; Dunlop, J.S.; Sanders, R.L.; Topping, M.W.; Reddy, N.A.; Amorín, R.; Begley, R.; Bolzonella, M.; et al. The NIRVANDELS Survey: A robust detection of α-enhancement in star-forming galaxies at z = 3.4. *Mon. Not. R. Astron. Soc.* **2021**, *505*, 903–920. [CrossRef]

67. Stanton, T.M.; Cullen, F.; McLure, R.J.; Shapley, A.E.; Arellano-Córdova, K.Z.; Begley, R.; Amorín, R.; Barrufet, L.; Calabrò, A.; Carnall, A.C.; et al. The NIRVANDELS survey: The stellar and gas-phase mass-metallicity relations of star-forming galaxies at z = 3.5. *Mon. Not. R. Astron. Soc.* **2024**, *532*, 3102–3119. [CrossRef]
68. Plat, A.; Charlot, S.; Bruzual, G.; Feltre, A.; Vidal-García, A.; Morisset, C.; Chevallard, J.; Todt, H. Constraints on the production and escape of ionizing radiation from the emission-line spectra of metal-poor star-forming galaxies. *Mon. Not. R. Astron. Soc.* **2019**, *490*, 978–1009. [CrossRef]
69. Sánchez, S.F.; Barrera-Ballesteros, J.K.; Lacerda, E.; Mejía-Narvaez, A.; Camps-Fariña, A.; Bruzual, G.; Espinosa-Ponce, C.; Rodríguez-Puebla, A.; Calette, A.R.; Ibarra-Medel, H.; et al. SDSS-IV MaNGA: PyPipe3D Analysis Release for 10,000 Galaxies. *Astrophys. J. Suppl. Ser.* **2022**, *262*, 36. [CrossRef]
70. Martins, F.; Palacios, A. Spectroscopic evolution of very massive stars at Z = 1/2.5 $Z_{\odot}$. *A&A* **2022**, *659*, A163. [CrossRef]
71. Hawcroft, C.; Leitherer, C.; Aranguré, O.; Chisholm, J.; Ekström, S.; Martinet, S.; Martins, L.P.; Meynet, G.; Morisset, C.; Sander, A.A.C.; et al. pySTARBURST99: The Next Generation of STARBURST99. *Astrophys. J. Suppl. Ser.* 2025, *submitted*.

Disclaimer/Publisher's Note: The statements, opinions and data contained in all publications are solely those of the individual author(s) and contributor(s) and not of MDPI and/or the editor(s). MDPI and/or the editor(s) disclaim responsibility for any injury to people or property resulting from any ideas, methods, instructions or products referred to in the content.